JOURNAL OF THERMOPHYSICS AND HEAT TRANSFER
Vol. 18, No. 1, January–March 2004

Technical Notes

TECHNICAL NOTES are short manuscripts describing new developments or important results of a preliminary nature. These Notes cannot exceed six manuscript pages and three figures; a page of text may be substituted for a figure and vice versa. After informal review by the editors, they may be published within a few months of the date of receipt. Style requirements are the same as for regular contributions (see inside back cover).

Direct Simulation of Free Molecular Flow in Fully Three-Dimensional Axial Rotor

S. M. Hosseinalipour* and A. Amoli†
Iran University of Science and Technology, 16765-163 Tehran, Iran
and
R. Ebrahimi‡
K. N. Toosi University of Technology, 16765-3381 Tehran, Iran

Nomenclature

A_p	=	passage area of rotor
b	=	blade chord
c	=	clearance between blade tip wall and casing
D	=	rotor diameter
h	=	radial distance between root and tip of blade
L	=	blade length
N	=	number of blades
p	=	pressure
Q	=	pumping speed per unit of molecular flux number incident upon the rotor, $W A_p$
R	=	radius
$\hat{R}$	=	gas constant
r	=	radial coordinate
s	=	blade spacing
T	=	temperature
t	=	time
U	=	blade speed ratio, $\omega R/(2\hat{R}T)^{1/2}$
v_r, v_θ, v_z	=	radial, tangential, and axial molecular velocity components
W	=	nondimensional pumping speed
w	=	blade thickness
z	=	axial coordinate
α	=	angle between the blade and line normal to the rotor axis
θ	=	azimuth angle
Σ	=	transmission coefficient
ψ	=	angle between symmetry planes of two adjacent blades, $2\pi/N$
ω	=	angular velocity of rotor

Subscripts

0	=	initial condition
1	=	upstream of rotor
2	=	downstream of rotor
m	=	midblade
r	=	root of blade
t	=	tip of blade

Introduction

THE pumping performance of turbomolecular pumps (TMPs) in free molecular flow has been investigated experimentally and theoretically by Kruger.[1] His study was based on parallel flat-plate blades with infinite height, and calculations were made on single-row and multirow blades by Monte Carlo methods. Sawada et al.[2] studied flat blades with finite height for a single rotor using an integration method. This method was based on some geometrical calculations for transmission of molecules from elements of the blade and integration of these elements on the blade boundary. However, a closed-form solution for integral equations could not be found due to the complication of multiple reflections between blades, and a solution was obtained using a numerical approach.

Katsimichas et al.[3] simulated free molecular flow within a single-rotor machine with a three-dimensional flat-plate blade using the Monte Carlo method. Their calculations were done in the rotational reference frame where the molecular paths were not straight lines; they also neglected effects of clearance between the tip of the blade and the pump casing. The maximum compression ratio was found higher than that calculated via two-dimensional simulation, especially at high rotational speed and when pumping heavy gases.

Skovorodko[4] considered the effect of clearance between the blade tip and pump casing. Neglecting the blade thickness, he simulated free molecular flow in a couple of rotor–stator stages using the inertial frame of reference and Monte Carlo method. In an inertial frame the moving path of a molecule is a straight line and following this path is done both in rotor and stator in a similar system of coordinates. This is actually one of the main advantages of using the inertial frame in such simulations. In the present work, the simulation of a single rotor with flat-plate blades is done considering three-dimensional and real topology of the system in an inertial frame of reference. The effects of both blade thickness and blade-casing clearance are also considered.

Numerical Approach

Figure 1 illustrates top and cross-sectional views of a single rotor. It can be shown that ultimate compression ratio and maximum nondimensional pumping speed of the rotor would be as follows[1,2]:

$$(p_2/p_1)_{\max} = \Sigma_{12}/\Sigma_{21}, \qquad W_{\max} = \Sigma_{12} - \Sigma_{21} \tag{1}$$

where W is defined as the net number of molecules that flow from upstream to downstream per unit area and per unit molecular flux number incident upstream of the blades. It is assumed that both inlet and outlet sides of the rotor face extremely large spaces and in these spaces molecules move with Maxwellian velocity distribution.

Received 30 April 2003; presented as Paper 2003-3777 at the AIAA 36th Thermophysics Conference, Orlando, FL, 23–26 June 2003; revision received 4 August 2003; accepted for publication 7 August 2003.

*Assistant Professor, Department of Mechanical Engineering; alipour@iust.ac.ir.
†Researcher, Department of Mechanical Engineering; ali_amoli@hotmail.com.
‡Assistant Professor, Department of Mechanical Engineering; Rebrahimi@kntu.ac.ir.

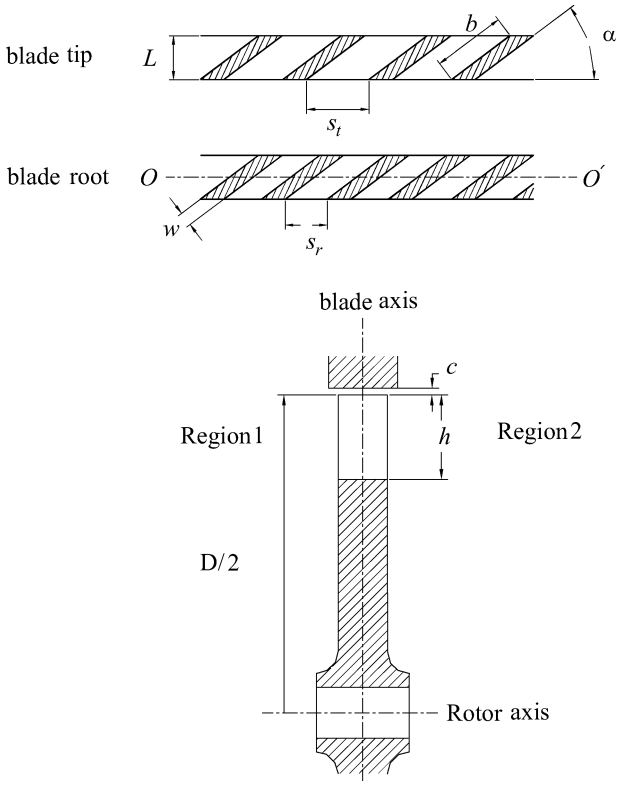

Fig. 1 Top view of blades and cross-sectional view of a single rotor.

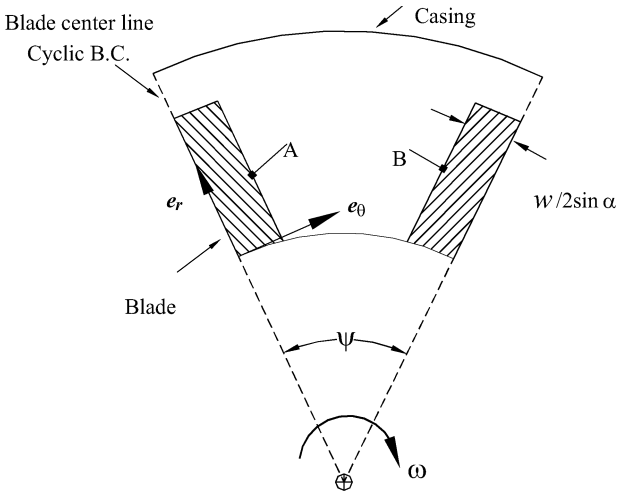

Fig. 2 Solution domain between two adjacent blades (at line OO′ in Fig. 1).

Then samples of molecules are entered individually in the blade row and each molecule is followed as it enters the passage, undergoes successive reflections, and finally emerges upstream or downstream. The fraction of all such molecules transmitted through the blade row from upstream (downstream) to downstream (upstream) gives the probability of transmission Σ_{12} (Σ_{21}).

In Fig. 2 the solution domain is shown for a single rotor row. This domain includes a channel between two adjacent blades that is symmetrically repeated around the periphery of the rotor body. As shown in Fig. 2, there are three types of boundary conditions: 1) a solid boundary that includes blade walls, rotor body, and casing; 2) cyclic boundary conditions that are the symmetric planes of each blade and are shown by dashed lines; and 3) inlet and outlet boundaries, which are planes that a molecule enters or emerges from and are surrounded by solid and cyclic boundaries. To perform an exact computation for collision of each molecule with each boundary surface, the analytical equations of these surfaces are needed. If one assumes that the central axis of the blade is perpendicular to the rotor axis, then the equations for the inside walls of the blades (planes A and B in Fig. 2) in a cylindrical coordinate system (r, θ, z) can be written as follows:[5]

Plane A:

$$r\sin(\theta-\omega t)\sin\alpha - z\cos\alpha - w/2 = 0 \tag{2}$$

Plane B:

$$r\sin(\theta-\psi-\omega t)\sin\alpha - z\cos\alpha + w/2 = 0 \tag{3}$$

It is noted that analytical equations of cyclic surfaces corresponding to planes A and B in Fig. 2 are like Eqs. (2) and (3) where w is equal to zero. The other boundaries in the solution domain include cylindrical surfaces such as rotor body, casing, and blade tip wall, which can be readily expressed in cylindrical system as $r = R_B$, where R_B is the radius of these surfaces. Also, by introducing the reference point at the middle of the blade chord, the inlet and outlet surfaces are expressed as $z = -L/2$ and $z = L/2$, respectively.

Neglecting intermolecular forces, the motion of a molecule through a rotor would occur in a straight line with the following equations:

$$\begin{aligned} r(t) &= \left[\left(v_{r_0}^2 + v_{\theta_0}^2\right)t^2 + 2r_0 v_{r_0} t + r_0^2\right]^{\frac{1}{2}} \\ \theta(t) &= \theta_0 + \arctan\left\{\left[\left(v_{r_0}^2 + v_{\theta_0}^2\right)t + r_0 v_{r_0}\right]\Big/ r_0 v_{\theta_0}\right\} \\ &\quad - \arctan\left(v_{r_0}\Big/ v_{\theta_0}\right) \\ z(t) &= z_0 + v_{z_0} t \end{aligned} \tag{4}$$

where (r_0, θ_0, z_0) and $(v_{r_0}, v_{\theta_0}, v_{z_0})$ present initial coordinates and initial velocity of molecules at the entrance of the blade or when the molecule is reemitted from solid surfaces. Also, the radial, tangential, and axial velocity components of the motion of a molecule in a cylindrical coordinate system can be expressed as follows:

$$\begin{aligned} v_r(t) &= \left[\left(v_{r_0}^2 + v_{\theta_0}^2\right)t + r_0 v_{r_0}\right]\Big/ r(t) \\ v_\theta(t) &= r_0 v_{\theta_0}/r(t) \\ v_z(t) &= v_{z_0} \end{aligned} \tag{5}$$

Assuming a uniform distribution for the molecules at the inlet of the rotor row, the initial position of a molecule in cylindrical coordinates can be written in terms of random numbers (R_f) as follows:

$$\begin{aligned} r_0 &= \left[R_r^2 + R_f\left(R_t^2 - R_r^2\right)\right]^{\frac{1}{2}} \\ \theta_0 &= \zeta_A + R_f(\zeta_B - \zeta_A) \\ z_0 &= -L/2 \end{aligned} \tag{6}$$

where ζ_A and ζ_B are calculated from the solution of Eqs. (2) and (3) for θ at $t = 0$, $r = r_0$, and $z = z_0$ for each of the A and B planes.

The initial velocity components of the molecules entering the blade row can be written in terms of random numbers from molecular flux distribution function as[6]

$$\begin{aligned} v_{r_0} &= \rho\cos\phi \\ v_{\theta_0} &= \rho\sin\phi \\ v_{z_0} &= (-\ell_n R_f)^{\frac{1}{2}} \end{aligned} \tag{7}$$

where $\rho = (-\ell_n R_f)^{1/2}$ and $\phi = 2\pi R_f$. In Eqs. (7), velocity components are nondimensionlized using $(2\hat{R}T)^{1/2}$ as the most probable velocity. By introducing the equations of the trajectories of molecules into the analytical equations of the blade walls, the intersection point of the molecular path with the blade walls can be found. For instance, Eq. (3) can be rearranged as follows:

$$\theta(t) - \omega t - \psi - \arcsin\{[z(t)\cos\alpha - w/2]/[r(t)\sin\alpha]\} = 0 \tag{8}$$

Replacing $r(t)$, $\theta(t)$, and $z(t)$ from Eq. (4) into Eq. (8) yields a complicated equation for t. An appropriate numerical approach, like a bisection method, can be applied to solve this equation.

The reemission of molecules from solid surfaces is assumed fully diffusive, which means the direction of emission is independent of the direction of incidence. For those molecules that are reemitted from moving parts of the blade row, reflected tangential velocity is superimposed by angular velocity of the rotor. When a molecule leaves the cyclic boundary, it returns from another one with the same velocity components. A similar procedure is applied for calculation of the transmission coefficient Σ_{21}, which has to be replaced by $-\omega$ in the preceding equations.

Results

Numerical validation of the present algorithm is verified by comparing its results with the two-dimensional numerical results of Kruger for a single rotor.[1] The geometrical parameters of this rotor are given in Table 1 as rotor 1. To have a near two-dimensional passage for this rotor, it is assumed that it has a very large diameter (e.g., $D/b = 500$ with appropriate blade numbers) and relatively large height (e.g., $h/b = 10$) to omit the effects of rotor body and casing. Other geometrical parameters are kept as the original values in Table 1. Figure 3 shows variation of ultimate compression ratio with blade speed ratio at mean radius for rotor 1. As it is seen in this figure both of our modified results for two-dimensional passage and Kruger numerical results are coincident for all speed ratios.

The simulation results for the fully three-dimensional geometry of rotor 1 is also depicted in Fig. 3 as a solid line. The simulations were performed using different numbers of sample molecules (for each side of the rotor) ranging from 5×10^5 to 10^7. It was found that the ultimate compression ratio for the values higher than 5×10^6 remained within $\pm 2\%$ of the corresponding results. According to this observation all presented results for this case are based on this number of sample molecules.

The symbols in Fig. 3 represent the experimental data of rotor 1 obtained by Kruger for air and Freon 114. These experiments were done for downstream pressures in which free molecular flow existed for the entire passage of the blades.[1] The present fully three-dimensional numerical results in Fig. 3 show a very good agreement with experimental data of air. The maximum difference between simulation results and those of experimental data do not exceed 4.5%. However, there are large discrepancies between our fully three-dimensional results and the experimental data for Freon 114. According to Kruger, the main reason for these discrepancies is due to the fact that no ionization gauge calibration had been available; it was assumed that the gauge response would be linear with density changes.[7] Therefore, the Freon 114 experimental data seem to be inadequate.

Table 1 Geometrical parameters of four single rotors

Parameter	Rotor 1	Rotor 2	Rotor 3	Rotor 4
N	25	24	36	48
D, mm	185.4	180	180	180
b, mm	37.1	23.4	16	12.4
α, deg	20	20	30	40
s_r, mm	14	9.5	6.4	4.9
s_t, mm	20.5	14.3	9.5	7.2
w, mm	0.94	0.8	2.3	2.9
h, mm	28	18	18	18
c, mm	0.3	0.3	0.3	0.3

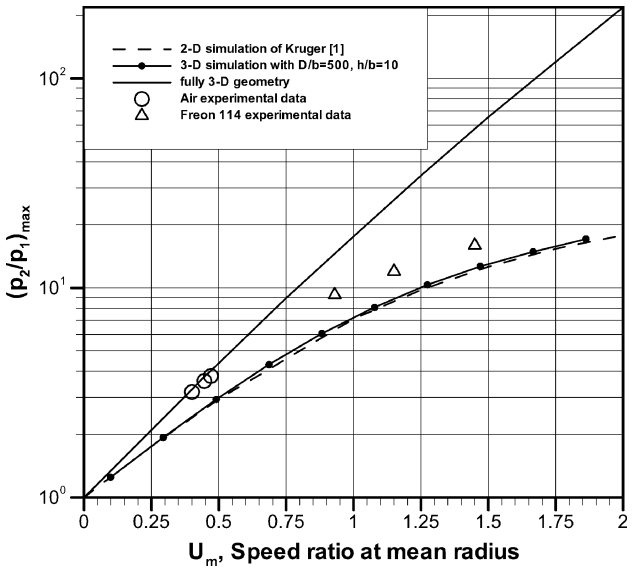

Fig. 3 Variation of ultimate compression ratio with blade speed ratio for Kruger's[1] rotor.

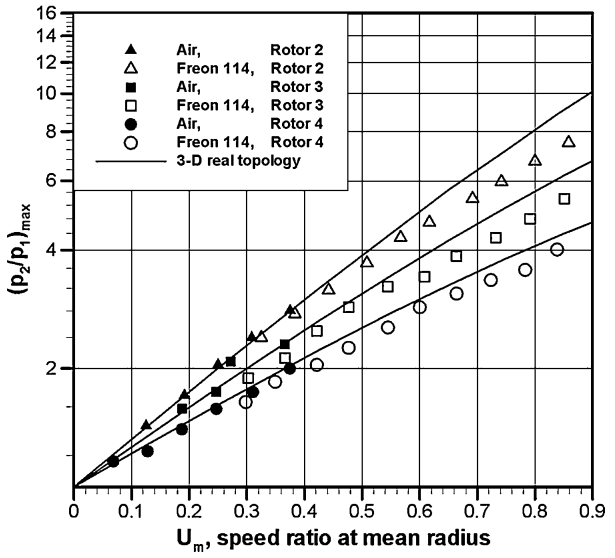

Fig. 4 Variation of ultimate compression ratio with blade speed ratio for rotors studied by Sawada.[2]

The difference between two-dimensional simulation results and fully three-dimensional ones is also noticeable in Fig. 3. This figure shows that for all speed ratios the two-dimensional simulation underestimates the compression ratio and the difference between three- and two-dimensional results becomes more pronounced in higher rotational velocities. This is also true when one uses TMPs for heavy or cold gases.

Figure 4 depicts the experimental data of Sawada[2] for variation of ultimate compression ratio with blade speed ratio for three rotors with blade angles of 20, 30, and 40 deg, respectively. The other geometrical parameters of these rotors are given in Table 1 as rotor 2, rotor 3, and rotor 4. The spacing of these rotors at mean radius is approximately equal to 0.5; Fig. 4 represents the effects of blade angle on compression ratio. As shown, at a constant blade speed ratio, the compression ratio increases when the blade angle decreases. The numerical results obtained by the present simulation are also given in this figure. Good agreement between experimental data and calculated results for both air and Freon 114 confirms the validation of these simulations.

Using the parametric study, accompanied by some appropriate nondimensional parameters of a single rotor, one can gain a good insight to both performance analysis and optimum design procedure for multistage TMPs. In this regard the following parameters are introduced as appropriate geometrical nondimensional parameters: angle of blades α, D/b, h/b, w/b, c/b, and finally s_m/b, which can be related to each other via the following equation:

$$\pi(D/b - h/b) = N(s_m/b + w/b \sin\alpha) \tag{9}$$

Considering D/b, w/b, and c/b as the design conditions, numerous simulations are performed for various sets of α, s_m/b, and h/b (Fig. 5). Each broken line in this figure performs the corresponding highest compression ratio for a certain pumping speed. As explained in Ref. 8, a rough estimation of blade arrangements for multirow TMPs can be obtained using this curve as the design.

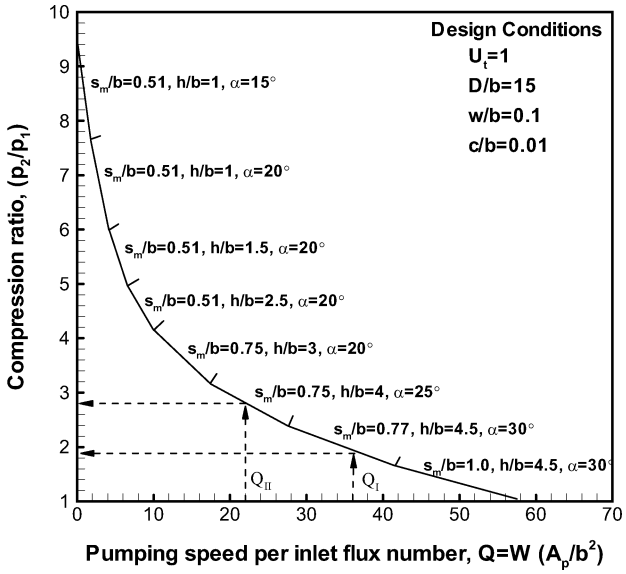

Fig. 5 The design curve for a single rotor.

Let Q_1 be the desired pumping speed at the first stage of a multirow TMP with design conditions as presented in Fig. 5. The values of compression ratio, blade angle, s_m/b, and h/b for this stage are suggested by the design curve using the following procedure. Using continuity, the pumping speed for next stage is found as $Q_1 = Q_{11}/(p_2/p_1)$ and the design curve yields the compression ratio and blade characteristics for next stage. The same steps can be used in order to find the suitable values of α, s_m/b, and h/b for next stages. As can be seen in Fig. 5, the blades of the first stages should have large angle, large heights, and great spacing-to-chord ratios, whereas for rear stages, blades with small angles, small heights, and small spacing-to-chord ratios are suitable.

Conclusions

The pumping performance of a single axial rotor in free molecular flow is investigated considering real topology of the flow passages. Good agreement between the presented method and known experimental data confirms the validity of the simulation. The parametric study for numerous sets of blade geometry yields a design curve that suggests optimum compression ratio or pumping speed for the desired conditions. The design curve shows that, for maximum pumping speed, the prior stages of a TMP should have blades with wide spacing, large height, and large angle, whereas the later stages should to be designed with small height, small angle, and small spacing.

References

[1]Kruger, C. H., and Shapiro, A. H., "The Axial-Flow Compressor in the Free-Molecule Range," *Proceedings of 2nd International Symposium on Rarefied Gas Dynamics*, Academic Press, New York, 1961, pp. 117–140.

[2]Sawada, T., Suzuki, M., and Taniguchi, O., "The Axial Flow Molecular Pump, 1st Report, on a Rotor with a Single Blade Row," Institute of Physical and Chemical Research, Japan, Vol. 62, No. 2, 1968, pp. 49–64.

[3]Katsimichas, S., Goddard, A. J. H., Lewington, R., and de Oliveira, C. R. E., "General Geometry Calculations of One-Stage Molecular Flow Transmission Probabilities for Turbomolecular Pumps," *Journal of Vacuum Science and Technology*, Vol. 13, No. 6, 1995, pp. 2954–2961.

[4]Skovorodko, P. A., "The Topology of Molecular Flow in Axial Compressor," *47th AVS International Symposium: Vacuum, Thin Films, Surfaces/Interfaces and Processing*, American Vacuum Society, New York, Oct. 2000, p. 155.

[5]Amoli, A., Hosseinalipour, S. M., and Ebrahimi, R., "Direct Simulation of Free Molecular Flow in Fully 3-D Axial Rotor," AIAA Paper 2003-3777, June 2003.

[6]Bird, G. A., *Molecular Gas Dynamics and the Direct Simulation of Gas Flows*, 2nd ed., Oxford Univ. Press, New York, 1994.

[7]Kruger, C. H., "The Axial-Flow Compressor in the Free-Molecule Range, Ph.D. Dissertation, Dept. of Mechanical Engineering, Massachusetts Inst. of Technology, Feb. 1960.

[8]Sawada, T., and Taniguchi, O., "The Axial Flow Molecular Pump, 3rd Report, Trial Manufacture and Performance Test," *Bulletin of the Japan Society of Mechanical Engineers*, Vol. 16, No. 92, 1973, pp. 312–318.

Backward Monte Carlo Method Based on Radiation Distribution Factor

L. H. Liu*
Harbin Institute of Technology,
150001 Harbin, People's Republic of China

Introduction

MONTE Carlo method simulates radiative transfer by tracing the histories of a number of rays that represent photon bundles traveling through the medium.[1,2] There are two types of Monte Carlo methods, namely, the forward Monte Carlo method and the backward (or reverse) Monte Carlo method. Forward Monte Carlo methods simulate a history of photon bundle starting at emission and ending at absorption, determining how much radiation power is transferred from one region to another. Backward Monte Carlo methods start at a termination site, for example, detector, and trace the photon bundle in the reverse direction, determining how much radiation power emitting along the path is incident on the termination site. For a measurement problem, using forward Monte Carlo simulation, one would emit and trace many photon bundles, even though only the tiniest of fraction will hit the detector. In this case, forward Monte Carlo simulation can become terribly inefficient. However, backward Monte Carlo simulation can alleviate this problem.

The backward Monte Carlo technique is based on the principle of reciprocity in radiative transfer theory as described by Case.[3] Walters and Buckius[4] developed a comprehensive reverse Monte Carlo method for computing the emission of a generalized enclosure containing an absorbing, emitting, and scattering medium. Modest[5] gave a comprehensive formulation for backward Monte Carlo simulation, capable of treat emitting, absorbing, and anisotropically scattering media with collimated irradiation, point, or line sources. If the temperature or the collimated irradiation are changed, even if the absorption and scattering coefficients of medium do not depend on temperature, backward Monte Carlo techniques of Walters and Buckius[4] and Modest[5] need to restart to trace all photon bundles from the beginning. Sometimes, this will suppress the efficiency of these methods, especially for inverse analysis of temperature field by using the outgoing emission intensity through a pore on the boundary of enclosure. This problem can be overcome by using the concept of radiation distribution factor[6] in the case that the radiative properties of medium and boundary do not depend on temperature.

The objective of this Note is to develop a backward Monte Carlo method based on the concept of radiation distribution factor and extend it to the cases with collimated irradiation, point, or line sources. A same example used by Modest[5] is applied to verify this new strategy.

Mathematical Formulation

As shown in Fig. 1, a three-dimensional semitransparent gray absorbing-emitting-scattering medium is bounded by connected

Received 19 May 2003; revision received 8 August 2003; accepted for publication 2 September 2003.

*Professor, School of Energy Science and Engineering, 92 West Dazhi Street; liulh_hit@263.net.